PFC/JA-86-53

Stabilization of MHD Modes in an Axisymmetric Plasma Column Through the Use of a Magnetic Divertor

Kesner, J., Lane, B., Post, R.S.

Plasma Fusion Center
Massachusetts Institute of Technology
Cambridge, MA 02139

April, 1986

To be published in: Nuclear Fusion

This is a revision of report PFC/CP-85-5 under the same title

Abstract

In order to stabilize MHD interchange modes in the central cell of a tandem mirror we propose the introduction of a magnetic limiter. The magnetic limiter creates a ring null in the magnetic field and electrons which enter the null can stream azimuthally and thereby "short-circuit" m = 1 fluctuations. This disallows a rigid m = 1 response and introduces finite Larmor radius stabilization effects in much the same fashion that they appear for higher azimuthal modes. Some pressure gradient can be maintained on the separatrix flux surface by locating the null on a local magnetic maxima. This scheme introduces the possibility of a fully axisymmetric tandem mirror.

I. Introduction

Axisymmetry is desirable in tandem mirror and other confinement devices from the point of view of improved equilibrium and reduced radial transport as well as less stringent engineering constraints. To this end, several partially axisymmetric schemes are being explored in tandem mirrors. The TARA[1] experiment at MIT locates a quadrupole cell at the ends of the device, beyond the axisymmetric confinement region. The Gamma-10[2] experiment in Tsukuba, Japan, locates quadrupole cells before the axisymmetric plugs. The former device may be more susceptible to trapped particle modes, the latter to radial transport.

The fluctuations that are observed in presently operating tandem mirrors appear to primarily exhibit an azimuthal mode number, m, of m = 1[3,4]. It is believed that higher mode numbers are stabilized by finite Larmor radius (termed FLR) effects. Thus the problem of obtaining stability of MHD and trapped particle instabilities can be reduced to the stabilization of m = 1 modes, which characteristically exhibit rigid radial perturbations.

In this paper we describe a new approach to obtaining stability without disturbing the axisymmetry of a tandem mirror. This would involve creation of an axisymmetric field null located axially within the central cell and on the flux tube, which corresponds to the edge of the hot core. (The null falls on a magnetic field separatrix, and field lines beyond the null are diverted). We show schematically in Fig (1) the central cell of the Tara experiment modified to include the magnetic divertor. The null is located on a local field maxima adjacent to the main gas box so that some fraction of the hot particles on the field lines that intersect the null can be magnetically confined and partially isolated from the null and gas box region. Ions which suffer non-adiabatic changes in magnetic moment as they pass near the null are confined by potential barriers in the plugs at either end of the center cell.

The effect of the null is to allow electrons within a layer an electron Larmor radii thick centered about the null flux tube to stream azimuthally in an incoherent fashion during a wave period. The electrons in this layer exhibit a Boltzmann response to a potential perturbation similar to passing electrons on an irrational surface in a tokamak configuration. Ions whose orbits pass through the electron layer also suffer non-adiabatic jumps in pitch angle if they pass through the null, but in general their azimuthal drifts are not appreciable during a wave period. The bulk of the ions respond to a flute-like electrostatic mode by E×B drifting in perturbed fields. Thus, in the electron non-adiabatic layer, quasi-neutrality requires an electron drift wave. Within the core of the plasma, both electrons and ions exhibit the usual response of a magnetized plasma. Both species E×B drift (to lowest order)in the perturbed electrostatic potential and quasi-neutrality is determined by balancing the residual non-cancellations in the perturbed drifts. These non-cancellations arise from the ion polarization drift, the averaging of the potential over an ion Larmor orbit and the Doppler shifts due to the curvature drifts. Because the first two arise from the finite ion orbits, they determine the radial structure of the mode. In general, the spectrum of eigenfrequencies, ω_n, obtained by imposing physical boundary conditions on the perturbed potential in the core does not match the eigenfrequency necessary to obtain quasi-neutrality in the electron non-adiabatic layer. Thus, the plasma exhibits two localized modes: a drift wave localized in the electron layer and a curvature driven interchange mode which extends through the core and vanishes on the null flux tube. The stability of the latter is determined by the competition of the curvature drive with the finite Larmor radius (FLR) terms. The FLR stabilizing terms are minimized by eigenfunctions which are rigid. Since the mode must vanish at the null flux surface, the eigenfunction cannot be rigid over the entire column. The global stability of the mode is determined quantitatively by plasma parameters and profiles. When the $m = 1$ mode is stabilized by FLR effects, higher azimuthal mode number perturbations, which are more strongly affected by FLR, are also stable.

The divertor null can be viewed as analogous to a line-tying region with the following important difference: for line-tying to a non-emitting end wall, a sheath forms at the wall so as to maintain field line neutrality. The sheath adds a resistive response which reduces the efficiency of the line-tying. With the divertor, all of the electrons that stream into the divertor null also leave so that no space charge sheath appears and the response is not resistive. Thus the magnetic divertor can be thought of as an electron-emitting line-tying element.

II. Magnetic Divertor Design and Particle Orbits

a. Field Structure

For simplicity we consider adding the magnetic divertor to the midplane of the central cell of a tandem mirror. (In principle, more than one such divertor can be utilized, for example at each end of the central cell). Fig. 1 displays schematically the axial magnetic field for a tandem mirror. The central cell, including the midplane magnetic divertor and the axisymmetric end plugs are shown. Fig. 2 shows an expanded view of the midplane magnetic field structure obtained from the EFFI Code[5]. Notice that 3 coils have been added to the coil set to create the divertor field structure. The three coil arrangement is relatively simple and allows the null position to be moved, but has the disadvantage that some plasma scrapes-off on the central coil leads and supports from the plasma beyond the separatrix. The power drain associated with this loss can be made small compared with the power input to the plasma core for a properly designed system.

b. Orbits in the Null

Electrons which enter into the vicinity of the null will become trapped in the null, stream azimuthally and re-emerge at a random azimuthal as well as pitch angle. This process can be understood as follows: When the electron gyro-radius equals the magnetic field gradient the electrons become non-magnetized. For a 100 eV electron, loss of adiabaticity occurs about 1 cm from the null in our design, at a magnetic field of approximately 200 G. While an electron is in this region it will then stream both axially and azimuthally across the null. As the electron re-enters the region of B > 200 G it becomes adiabatic with a random pitch angle. However, since the magnetic field rises up to 5 KG, the electron finds itself in a magnetic well with a mirror ratio of 25 and has only a $1/2R \sim 2\%$ chance of escaping. Thus it will "rattle" around the null about 50 times before escaping. If a group of electrons of different initial pitch angles and gyrophases is started at one point on a field line passing through the null, during a wave period the group will spread incoherently over the null flux surface.

Exact electron orbits have been studied numerically. From these orbits we observe that the azimuthal drift on each passage through the null is unidirectional. Electrons below the separatrix stream in the bad curvature drift direction and above in the good curvature direction. This result is shown analytically in Appendix A. The implication of this fact is that the azimuthal streaming is proportional to the number of passages through the null before escaping.

III. Stability Analysis

a. Equilibrium

We consider an equilibrium as shown in Fig 3 where the plasma pressure vanishes just beyond the null flux tube and the plasma density extends beyond this flux tube. We assume the pressure to nearly vanish on the null flux tube because ions that cross the null have the possibility of passing along the field lines that circle the conductor. Some of those particles will be lost on the support leads while other ions will be exposed to charge exchange on gas since the plasma is thin at this point. We expect, however, that due to ionization of ambient gas a cooler plasma (10 - 100 eV) will be maintained on field lines outside the null flux tube. The density of this cooler plasma will depend on the axial and radial confinement, the edge neutral density and the power available at the edge to maintain the electron and ion temperatures. We turn now to the perturbation analysis.

b. Perturbation Analysis - Effect of Electron Layer

We divide the plasma into four radial layers as shown in Fig. 4: the electron non-adiabatic layer, the ion non-adiabatic layer, a transition layer and the core. In the remainder of the text the first two will be referred to as the electron and ion layer. In the electron layer the electron dynamics is dominated by the null which allows electrons to stream across the field. The electron response in both the ion layer and the core, however, involves cross-field drifts under the influence of the perturbing electric fields. The ion response throughout the plasma is non-local due to the integration of the radial potential structure along an ion's Larmor orbit. We address the implications of this below. In addition, the loss of adiabaticity for null passing ions influences the ion parallel dynamics. In the core, both electrons and ions are magnetized and the mode structure is governed by the familiar Rosenbluth and Simon finite Larmor radius differential equation[6,7] modified to allow for transiting electrons. These equations exhibit a mode driven by the plasma pressure gradient and the unfavorable curvature of the confining field. We wish to consider the stability of this curvature driven mode driven by the core pressure gradient in the presence of a magnetic limiter. We assume throughout that the plasma beta, $\beta \equiv 8\pi P/B^2$, is small enough that electromagnetic effects can be neglected. Thus, all perturbations are assumed to arise from the perturbed electrostatic potential $\tilde{\phi}$.

Several possible behaviors of $\tilde{\phi}$ in the vicinity of the electron layer must be considered. The first is that the flute mode from the core extends continuously through the electron layer as if the layer did not exist. We will argue that such a radial mode structure violates quasi-neutrality in the electron layer. The second is that the mode varies rapidly within a few Larmor radii of the electron layer and evades the finite Larmor radius stabilization that one would expect to accompany such a rapid variation in the eigenfunction. We will argue that such a solution cannot match smoothly to a core solution due to the non-local nature of the ion response and further violates quasi-neutrality in the electron layer. We conclude, therefore, that the only self-consistant solution is for the eigenfunction for the core perturbation to vanish smoothly within approximately two cold ion Larmor radii of the null flux tube.

In order to illustrate the basic physics behind this reasoning, we simplify the calculation in the vicinity of the null flux tube by assuming a slab plasma with a constant magnetic field $\underset{\sim}{B} = B_0\hat{z}$, and equilibrium gradients in pressure and density only along x. We model the effect of curvature by a species dependent gravity $g\hat{x}$ ($g \equiv (v_\perp^2/2 + v_{||}^2)/R_c$, $R_c \equiv$ radius of curvature). We assume no variation in equilibrium or perturbed quantities along z and no equilibrium electric field and consider electrostatic perturbations $\tilde{\phi} = \phi(x)\exp(ik_y y - i\omega t)$. Under these assumptions we can solve the Vlasov equation by integration along characteristics under the assumption $\omega \ll \Omega$ and $|k_y\rho_i| < |\rho_i\, \partial/\partial x|$ with ω, k_y the wave frequency and wave number, Ω the ion cyclotron frequency, and ρ_i the ion gyroradius.

This yields

$$f_i \simeq q\phi\frac{\partial F_0}{\partial \epsilon} - \left(q\,\frac{\partial F_0}{\partial \epsilon} + \frac{k_y c}{\omega B}\,\frac{\partial F_0}{\partial x_{gc}}\right)\langle\phi\rangle_{\rho_i} \tag{1}$$

where

$$\langle\phi\rangle_{\rho_i} = \frac{\Omega}{2\pi}\int_0^{2\pi/\Omega} d\tau\; \phi(\hat{x}(\tau),\, \hat{y}\,(\tau),\, \tau)$$

$$x_{gc} = x + \frac{v_\perp}{\Omega}\sin\psi = x + \frac{v_y}{\Omega}$$

$$\hat{x}(\tau) = x - \frac{v_\perp}{\Omega}\sin(\psi - \Omega\tau) + \frac{v_\perp}{\Omega}\sin\psi$$

$$\hat{y}(\tau) = y + \frac{v_\perp}{\Omega}\cos(\psi - \Omega\tau) - \frac{v_\perp}{\Omega}\cos\psi - \frac{g}{\Omega}\tau$$

$$F_0 = (\epsilon, x_{gc}). \tag{2}$$

$$\epsilon = 1/2\, mv_\perp^2 + 1/2\, mv_{||}^2$$

The quantity x_{gc} is the guiding center location of the particle and ψ is the phase angle. Integrating over velocity gives the perturbed ion response:

$$\tilde{n}_i = \{ \frac{\partial F_0}{\partial \epsilon} q\,(\phi - \langle\phi\rangle_{\rho_i}) \}_M - \frac{k_y c}{\omega B}\{ \langle\phi\rangle_{\rho_i} \frac{\partial F_0}{\partial x_{gc}} \}_M$$

$$- \frac{k_y^2 c^2}{\omega^2 q B^2}\,\kappa\,\{(mv_\perp^2/2 + mv_{||}^2)\,\frac{\partial F_0}{\partial x_{gc}}\,\phi\}_M \tag{3}$$

where $\{\bullet\}_M$ means an integration over a Maxwellian in energy and κ is the mean curvature ($\kappa \sim 1/R_c$).

Assuming that $\rho_i\, \partial F_0/\partial x_{gc} < F_0$ and that we can write $\phi = \phi_0\,(1 + x/L_1 + x^2/L_2^2)$, Eq. (3) yields the ion response calculated by Rosenbluth and Simon,[6,7]

$$\tilde{n}_i = - \frac{k_y c}{\omega B}\,\phi\,\frac{dn}{dx} + \frac{1}{2}\,\frac{m_i c^2}{qB^2}\left[\frac{d}{dx}\left[n\left(1 - \frac{k_y c}{q\omega B n}\frac{dP}{dx}\right)\frac{d\phi}{dx}\right] - k_y^2 n\left(1 - \frac{k_y c}{q\omega B n}\frac{dP}{dx}\right)\,\phi\right.$$

$$+ \frac{k_y^2}{\omega^2} \hat{g} \frac{dn}{dx} \phi \Bigg] \qquad (4)$$

where $\hat{g} \equiv 2T/(mRc)$. Thus in the core where scale lengths are larger than an ion Larmor radius, the integral and differential formulations of the ion response agree.

We wish now to examine the possible behavior of ϕ within a few Larmor radii of the electron layer. We note that the ion response at a point x depends on the perturbed potential between $x-2\rho_i$ and $x+2\rho_i$ due to the finite ion orbit. We consider an m = 1 eigenfunction with the fewest radial nodes. In the core we combine the ion response, Eq. (4) with the electron response outside the electron layer,

$$f_e = - \frac{k_y c}{\omega B} \frac{\partial F_0}{\partial x} \phi \qquad (5)$$

to obtain the Rosenbluth and Simon equations for a slab:[6,7]

$$\frac{d}{dx}\left[n\, \omega\left(\omega - \frac{k_y c}{qBn}\frac{dP}{dx}\right)\frac{d\phi}{dx}\right] - \omega\left(\omega - \frac{k_y c}{qBn}\frac{dP}{dx}\right)k_y^2 n + k_y^2 \hat{g}\frac{dn}{dx} = 0 \qquad (6)$$

We consider modes with $k_y \simeq r_p^{-1}$ and define $\omega_* \equiv (k_y c/qBn)\, dP/dx$ and $\gamma_{MHD}^2 \equiv \hat{g}\, d(\ln n)/dx$. If $\omega \sim \omega_* \sim \gamma_{MHD} \sim v_{ti}/L_t$ ($L_t \equiv$ axial magnetic field scale length) and there are no sharp gradients in density or pressure the eigenfunction with fewest nodes must vary on the scale length of density,

L_n, or pressure, L_p, which we assume is comparable to r_p the plasma radius.

In the transition layer between the core and ion layers, contributions to the ion response come from the perturbed potential in the core and in the ion layer. In this case the quasi-neutrality condition is

$$0 = \{ \frac{\partial F_0}{\partial \epsilon} q (\phi - <\phi>_{\rho_i})\}_M + \frac{k_y c}{\omega B} \{ \phi \frac{\partial F_0^e}{\partial x} - <\phi>_{\rho_i} \frac{\partial F_0}{\partial x_{gc}} \}_M$$

$$- \frac{k_y^2 c^2 \kappa}{\omega^2 q B^2} \{(mv_\perp^2 + mv_{||}^2) \frac{\partial F_0}{\partial x_{gc}} <\phi>_{\rho_i} \}_M. \qquad (7)$$

If ϕ varies rapidly in the ion layer or the matching layer then $\phi - <\phi>_\rho \sim \phi$ and the first two terms are larger than the third term by the ratio $r^2/\rho_i^2 \, (\omega/\gamma_{MHD})^2$. By balancing the first two terms we obtain $\omega = (k_y cT/eBn)\, (\partial n/\partial x) \simeq \omega_*$. To satisfy a similar equation in the core ϕ must also vary rapicly there which implies that we do not have the lowest radial eigenmode wit no nodes. We thus conclude that ϕ varies on equilibrium scale lengths even in the ion layer.

We now consider the ion response in the ion and electron layers. We must allow for the possibility that the perturbed potential jumps abruptly to a new value, ϕ_e, in the electron layer. Since the width of this layer is approximately $2\rho_e$ the additional contribution to the ion orbit integral is of order $(\phi_e - \phi_0)(\rho_e/\rho_i) = (\phi_e - \phi_0)\,(m_e/m_i)^{1/2}$, where ϕ outside the layer has been expanded as $\phi = \phi_0\,(1 + x/L_1 + (x/L_2)^2)$ which is appropriate since we have concluded that ϕ varies on an equilibrium scale length. Thus in the ion layer, quasi-neutrality becomes

$$0 = + \frac{e\phi_0}{T}\left(\frac{v_\perp^{2t}}{L_2^2\,\Omega^2}\,n + \frac{\partial n}{\partial x}\left[\frac{1}{2}\,\frac{v_\perp^{2t}}{\Omega^2 L_1} + \frac{v_\perp^{2t}}{\Omega^2}\,\frac{x}{L_2^2}\right]\right) + \frac{e}{T}\,(\phi_e - \phi_0)\left(\frac{m_e}{m_i}\right)^{1/2} A(x)$$

$$- \frac{k_y c}{\omega B}\left[\phi_0\left(\frac{\partial n}{\partial x}\,\frac{v_\perp^{2t}}{L_2^2\Omega^2} + \frac{\partial^2 n}{\partial x^2}\left[\frac{1}{2}\,\frac{v_\perp^{2t}}{L_1\Omega^2} + \frac{v_\perp^{2t}x}{\Omega^2 L_2}\right]\right)\right.$$

$$\left. + \frac{\partial n}{\partial x}\,(\phi_e - \phi_0)\left(\frac{m_e}{m_i}\right)^{1/2} A(x)\right] + \left(\frac{k_y^2\,v_\perp^{2t}}{\Omega^2}\right)\frac{\hat{g}}{\omega^2}\,\frac{dn}{dx}\,\frac{e\phi_0}{T}\,. \qquad (8)$$

Where $A(x) \simeq 1$ and $v_\perp^{\,t}$ is the thermal speed, $v_\perp^{2t} = 2T/m_i$.

In the ion layer the terms $(v_\perp^{\,t}\backslash L_2\Omega)^2$ are of order $(\rho_i/L_n)^2$. For cool ions, 10-100 eV, $L_2 \simeq L_n \simeq 15$ cm and $B \simeq 2$ kG, we find $(v_\perp^{\,t}/L_2\Omega)^2 \simeq 1 \times 10^{-4}$ to 1×10^{-3}. Thus the term $(\phi_e - \phi_0)(m_e/m_i)^{1/2}$ is the dominant term in the equation and forces $\phi_e \simeq \phi_0$ or otherwise L_2 must vary more rapidly than L_n which we have seen as inconsistent with a smooth core solution.

In the electron layer the azimuthal streaming of the electrons leads to a purely Boltzmann response

$$f_e = q\phi_e \frac{\partial F_0}{\partial \epsilon} \quad . \tag{9}$$

Combined with the lowest order ion response this gives for quasi-neutrality in the electron layer

$$\begin{aligned} 0 &= - \frac{e\phi_e}{T_e} n - \frac{k_y c}{\omega B} \{ \langle\phi\rangle_{\rho_i} \frac{\partial F_0}{\partial x_{gc}} \}_M \\ &\simeq - \frac{e\phi_e}{T_e} n - \frac{k_y c}{\omega B} \left(\phi_0 \frac{\partial n}{\partial x} \left(1 + 0 \left(\frac{v_\perp^2}{L_n^2 \Omega^2} \right) \right) \right) \\ &\quad + \frac{e}{T} (\phi_e - \phi_0) \left(\frac{m_e}{m_i} \right)^{1/2} A(x) \quad . \end{aligned} \tag{10}$$

If $\phi_e \simeq \phi_0$ the electron layer quasi-neutrality becomes

$$0 \simeq - \frac{e\phi_e}{T_e} n_0 \left(1 + \frac{k_y c T_e}{e\omega B} \frac{\partial n}{\partial x} \right). \tag{11}$$

This requires ω to take on a particular value. If we now return to the core equations and examine the spectrum of eigenvalues for the mode vanishing at some wall position, we will find in general that the particular value of ω required for quasi-neutrality in the electron layer is not included. We conclude, therefore, that the only solution in the electron layer is that both ϕ_e and $\langle\phi\rangle_{\rho_i}$ vanish there. This is possible only if ϕ vanishes at $x = 2\rho_i^c$, because of the integral non-local ion response.

A more detailed treatment would have considered the finite geometry effects due to the cylindrical confinement volume, the special nature of the ion orbits which pass through the null and the possible variation of ϕ along a field line. We expect that the finite geometry effects will be small since the ion layer is small compared to the null radius. Although the correct orbits are complex and not the simple circular gyro-motion considered in our model, the essential point is that ion response is non-local and depends on the potential structure within approximately two Larmor radius of the location under consideration. We further note that the disparity in the electron response from inside to outside the electron layer along the entire length of the field line is correct in the exact divertor geometry since passing electrons communicate the effect of the null to the entire length of the null flux tube during a wave period. Thus, a mode which is isolated in the well region would still need to vanish within a few cold ion Larmor radii of the null flux tube. We note that in our model, all electrons were taken to be affected by the null. This is correct for the situation $\nu_e > \omega$. For the collisionless case, a more correct treatment would have taken into account that electrons trapped in the well have the usual magnetized perturbed ExB drifts and that only the passing particles are affected by the null. Since passing particles make up 30% of density for a mirror ratio of 2, the dominant mode in the electron layer is still a drift wave.

c. Perturbation Analysis - Core Response

We turn now to the stability of the core plasma. Because of their high bounce frequency, core electrons respond to the average E×B drift in the perturbed fields Doppler shifted by the equilibrium drifts, and obtain the response

$$f_e = -e\phi\frac{\partial F_0}{\partial \epsilon} + \frac{1}{\omega - \omega_d}\left(e\omega\frac{F_0}{\partial \epsilon} - mc\,\frac{\partial F_0}{\partial \alpha}\right)\bar{\phi}$$

$$\omega_d \equiv \underset{\sim}{k} \cdot \underset{\sim}{b} \times (mv_{||}^2 + mv_{\perp}^2/2)\ R_c\ . \qquad (12)$$

The over bar indicates a bounce average,

$$\phi = \frac{\int \frac{dl}{v_{||}}\,\phi}{\int \frac{dl}{v_{||}}}$$

The transit frequency for ions through the well is comparable to the mode frequency, while the transit frequency for ions between the mirror peaks on either side of the null is large compared to the mode frequency. We do not treat the ion bounce resonance effects here but instead take all ions to be cold. Thus, the ions respond by drifting in the local perturbed field.

Quasi-neutrality is then determined by the Rosenbluth and Simon equations modified to allow for the bounce averaged electron response.[8]

$$0 = \frac{2}{\alpha^{1/2}} \frac{\partial}{\partial\alpha} \left(S\omega^2 n\alpha^2 \frac{\partial}{\partial\alpha} \left(\frac{\phi}{\alpha^{1/2}} \right) \right) - S\omega^2\, n\, \frac{(m^2 - 1)}{2\alpha}\, \phi$$

$$+ \omega^2 \frac{\partial n}{\partial\alpha}\, \phi$$

$$+ \frac{2m^2}{m_i r R_c} \frac{\partial P}{\partial\alpha}\, \phi$$

$$+ \frac{\Omega_i}{c} \int d^3v\, \omega \left(e\omega \frac{\partial F_0}{\partial\epsilon} - mc \frac{\partial F_0}{\partial\alpha} \right) (\phi - \bar{\phi}) \qquad (13)$$

where

$$S\omega^2 = \omega^2 - \frac{\omega mc}{en} \frac{\partial P_{i\perp}}{\partial\alpha} \equiv \omega\, (\omega - \omega_*^i)$$

and α is the flux variable $d\alpha = B\, rdr$. The effects due to radial electric fields have been neglected. Examining the ratio of the last term which represents the electron response, to the first four terms which represent, respectively, the ion polarization drift terms, the finite ion orbit connections to the B drift and the MHD drive, we conclude that when $\phi = \bar{\phi}$ the last term is large by the ratio of $(L_n/L_{tot})\ (n_{pass}/n_0)\ (r_n^2/\rho_i^2) \simeq 20 - 30$. Thus to lowest order $\omega \simeq \omega_*^e \equiv -\, (m\, cT/en)\ (\partial n/\partial\alpha)$, a drift wave, unless the mode is flute like ($\phi \underset{\sim}{\sim} \bar{\phi}$). We will only examine the later modes in detail.

We calculate the dispersion relation for the flute by setting $\phi = \phi_0(\alpha) + \phi_1(\alpha, z)$ and integrating over the plasma flux tube. This gives

$$\int \frac{dl}{B^2} \left[\frac{2}{\alpha^{1/2}} \frac{\partial}{\partial\alpha} \left(n\alpha^2 \quad \omega^2 - \frac{\omega cm}{en} \quad \frac{\partial P_{i\perp}}{\partial\alpha} \right) \frac{\partial}{\partial\alpha} \left(\frac{\phi_0}{\alpha^{1/2}} \right) - S\omega^2 n \frac{(m^2-1)}{2\alpha} + \phi_0 \omega^2 \frac{\partial n}{\partial\alpha} \right.$$

$$\phi_0 \cdot$$

$$\left. + \frac{2m^2}{m_i r R_c} \frac{\partial P}{\partial\alpha} \phi_0 \right] = 0 \; . \qquad (14)$$

We study the nature of the solutions to this equation by assuming that n and P are constants along a field line. It is convenient to normalize the equation as follows:

$$\frac{\partial}{\partial\hat{\alpha}} \left(2\hat{n}\hat{\omega} \left(\hat{\omega} - \frac{1}{\hat{n}} \frac{\partial\hat{P}}{\partial\hat{\alpha}} \right) \hat{\alpha}^2 \frac{\partial\xi}{\partial\hat{\alpha}} \right) - \omega\left(\omega - \frac{1}{\hat{n}} \frac{\partial\hat{P}}{\partial\hat{\alpha}}\right)(m^2 - 1)\hat{n} \; \xi + \hat{\omega}^2 \; \hat{\alpha} \; \frac{\partial\hat{n}}{\partial\hat{\alpha}} \; \xi$$

$$+ m^2 \hat{\Gamma}^2 \; \hat{\alpha} \; \frac{\partial\hat{P}}{\partial\hat{\alpha}} \; \xi = 0 \qquad (15)$$

where

$$\hat{\alpha} \equiv \alpha/\alpha_{null}$$

$$n(\alpha) \equiv n(0) \; \hat{n} \; (\alpha)$$

$$P(\alpha) \equiv P(0) \; \hat{P} \; (\alpha)$$

$$T(\alpha) \equiv T(0) \; \hat{T} \; (\alpha)$$

$$\hat{n}(0) \equiv \hat{P}(0) = \hat{T} \; (0) = 1$$

$$\hat{\Gamma}^2 \equiv \frac{2T(0)}{m_i} \frac{\int \frac{dl}{B^2} \frac{1}{rR_c}}{\int \frac{dl}{B^2}} \left(\frac{cT(0)}{e\alpha_{null}}\right)^{-2} \propto \left< \frac{\gamma_{MHD}^2}{\omega_*^2} \right>$$

$$\hat{\omega}_* \equiv \hat{n}^{-1}(\partial\hat{P}/\partial\hat{\alpha}) = \frac{1}{n}\frac{\partial P}{\partial\alpha} \Big/ \frac{P(0)}{(n(0)\alpha_{null})} .$$

$$\xi \equiv \frac{\phi_0}{\alpha^{1/2}} .$$

The eigenfrequencies which result from imposing the boundary condition that ξ vanish at $\alpha = \alpha_{null}$ depend on the parameter $\hat{\Gamma}$ and the profiles $\hat{n}$, $\hat{P}$, $\hat{T}$ and $\hat{\omega}_* = \hat{n}^{-1}\ (\partial\hat{P}/\partial\hat{\alpha})$.

In Fig.(5) we show the complex $\hat{\omega}$ plane and the path of the two roots of $\hat{\omega}$ for the n=0 mode with no nodes as $\hat{\Gamma}$ is increased. The cross-hatched region on the real axis shows the range of $\hat{\omega}_*$ (notice $\hat{\omega}_*$ is negative). We find that two roots exist for $\hat{\Gamma} \ll 1$. The first is slightly less than zero and the second is slightly greater than max $\hat{\omega}_*$. As $\hat{\Gamma}$ is increased, the roots coalesce and instability appears.

We have performed a Nyquist analysis numerically to verify that no other unstable roots exist for values of $\hat{\Gamma}$ less than the marginally stable value of $\hat{\Gamma}$ for the n = 0 mode. In particular within the context of the basic Rosenbluth and Simon equation for flute modes given above, there are no instabilities associated with the singularity that appears inside the plasma if $\hat{\omega} = \hat{\omega}_*$.

The two roots for $\hat{\omega}$ for modes with one or more nodes follow qualitatively the same path emerging from the the origin and the maximum of $\hat{\omega}_*$, coalescing and moving off the real axis. These modes become unstable at a larger value of $\hat{\Gamma}$ than the n=0 marginal value. Thus the first mode to be destabilized is the mode with no nodes. We have, in addition, examined modes with mode number m greater than one. We find that they are more stable than the m = 1, n = 0 mode. Thus, the most stringent stability condition is that demanded by the m = 1, n = 0 mode.

Although the exact value of $\hat{\Gamma}$ at which the n=0 mode is marginally stable depends on the pressure profile we find that this value is particularly dependent on the value of $\hat{\omega}_*$ at the null flux tube. In Fig. (3) we show a particular pressure profile we have investigated. By varying the model parameters slightly we can vary $\hat{\omega}_*$ at the edge while not significantly affecting the pressure profile or the $\hat{\omega}_*$ profile in the bulk of the core. In Fig.(6-a) and Fig. (6-b) we show two such profiles of $\hat{\omega}_*$ and in Fig.(7) we show the marginal value of $\hat{\Gamma}$ as a function of $\hat{\omega}_*(\hat{\alpha}$ =

$1)/\hat{\omega}_*(\hat{\alpha} = 0)$. Points corresponding to the two profiles shown in Figs. (6-a and 6-b) are indicated. We note that the marginal stability curve has a knee when $\hat{\omega}_*$ at the null flux tube equals $\hat{\omega}_*$ at the center. We find that the eigenfunction for the more negative (stable) root turns over sharply near the minimum value of $|\hat{\omega}_*|$. In the case that $\hat{\omega}_*$ at the edge is less negative than $\hat{\omega}_*$ at the center, the eigenfunction extends through the core and turns over sharply near the null flux tube. In the case that $\hat{\omega}_*$ at the edge is more negative than the axis value the eigenfunction turns over rapidly near the axis and has a small value through the bulk of the core. In both cases the eigenfunction for the root nearer to the origin varies smoothly over the plasma core. The m = 2 mode picks up additional FLR stability and is stable when the m = 1 mode is stable.

In order to relate the numerical work above to experiments we note that $\hat{\Gamma}$ depends on the confinement geometry and scales as the inverse square root of T_i. For the Tara configuration $\hat{\Gamma}$ is approximately unity assuming an ion temperature of 100 eV and neglecting the effect of the hot ion population in the axisymmetric plugs. Thus stability to the m=1 mode will depend on the value of the pressure gradient near the plasma edge. A discussion of the details of the plasma equilibrium near the plasma edge will be considered in a subsequent paper. We note here that in the configuration proposed for the

Tara experiment the divertor is located on a local magnetic hill adjacent to the gas box which is the main gas source for the plasma. Ions are therefore partially magnetically confined in the well regions and are axially isolated from the region where the neutral gas pressure is highest. This configuration permits energetic ions to extend to the null flux tube.

III. Discussion and Conclusion

We propose a new stabilization scheme for electrostatic low frequency modes in an axisymmetric configuration using a magnetic ring divertor.

The proposed magnetic geometry bears a superficial resemblance to internal ring mirror devices[8] such as Surmac[9]. The proposed stabilization however, does not come from the good average curvature beyond the separatrix but from the tendency of the null to randomize the azimuth of passing electrons. (This randomization is much like the effect of the rotational transform on passing particles in tokamak trapped particle theory).

We have shown that the electron response in a thin layer about the null flux tube is the residual Boltzmann response. Quasi-neutrality can only be satisfied in this layer by an electron drift wave whose frequency is incompatible with the frequency of the core curvature driven interchange mode. Thus the core mode must vanish at the null flux tube. The stability of the core then depends on the competition between finite Larmor radius effects and curvature drive. Numerically we find that the key parameter is the value of the pressure gradient at the null flux tube. We propose to maintain a finite pressure gradient experimentally by isolating the gas source axially from the hot ions by mounting the gas box on a local magnetic hill.

We note that in some respects the stabilization mechanism proposed here is similar to line tying at the plasma edge or stabilization by the presence of a metal wall at the plasma edge. In contrast to line tying it is not necessary to employ either emitting walls or high edge neutral pressures usually associated with line tied plasmas. In contrast to a metal limiter we note that the presence of electrostatic sheaths at metal surfaces both parallel and perpendicular to field lines may allow electrostatic perturbations to extend with finite amplitude up to a few Debye lengths from the metal surface effectively isolating the core from the effects of the limiter.

Finally the magnetic divertor geometry permits greater control of the plasma edge region since the diverted plasma can be fueled and heated separately from the bulk plasma. Such control would lead to additional benefits in the form of additional core shielding from neutral gas and impurities.

Appendix A - Orbits in Null Region

To obtain the orbit equations for particles entering the null we start with the Lagrangian:

$$L = \frac{1}{2} m (r\dot{\theta})^2 + \frac{1}{2} m\dot{r}^2 + \frac{1}{2} m\dot{z}^2 + \frac{q_e}{c} A_\theta(r,z)\, r\dot{\theta}. \qquad \text{(A1)}$$

Due to axisymmetry the system does depend on the azimuthal variable, θ. Applying the Euler-Lagrange equation

$$\frac{d}{dt}\left(\frac{\partial L}{\partial \dot{q}_j}\right) - \frac{\partial L}{\partial q_j} = 0 \qquad \text{(A2)}$$

and defining the flux function to be

$$\Psi \equiv rA_\theta = \frac{1}{2\pi}\int \underset{\sim}{B} \bullet \underset{\sim}{da} \qquad \text{(A3)}$$

We can obtain the equations of motion

$$0 = \ddot{r} + \frac{\partial}{\partial r}\Phi \qquad \text{(A4a)}$$

$$0 = \ddot{z} + \frac{\partial}{\partial z}\Phi \qquad \text{(A4b)}$$

and

$$r\dot{\theta} = \frac{e}{mcr}(\Psi - \Psi_o) \qquad \text{(A4c)}$$

where we have defined a pseudo-potential

$$\Phi \equiv \frac{e^2}{2m^2c^2}\left[\frac{\Psi - \Psi_o}{r}\right]^2. \qquad \text{(A4d)}$$

Ψ_0 is the mean flux value of the particle orbit defined by zero instantaneous azimuthal velocity, $\dot{\theta}$.

The particle motion in r and z is thus reduced to the analogous motion of a ball in the potential Φ. In a region of uniform magnetic fields, this potential resembles a trough in which the particle executes a bouncing motion perpendicular to the field and a streaming motion parallel to the field. Note that Ψ is a constant along a field line and that Ψ_0 is a constant of the motion. Thus as the magnetic field decreases in strength, the radial position of the minimum of the potential moves outward and the pseudo-potential becomes shallower corresponding to the decreasing cyclotron frequency.

At the field null, the pseudo-potential has a saddle point. Thus a particle whose "gyro-center" Ψ_0 lies close to Ψ_{null} can pass over the saddle [illegible] out of the null along [illegible] field line that encircles the [illegible]ng the null. The stre[illegible]ming motion in θ results from the [illegible]es which "linger" near th[illegible] top of the saddle. Recalling that $r\dot{\theta} = e/(mcr)\ (\Psi - \Psi_0)$, one can see that an electron whose "gyro-center" Ψ_0 is less than Ψ_{null} will always stream in the same direction due to the particle "lingering" at the null saddle point. This streaming, in fact, goes over to the usual curvature drift for particles whose "gyro-centers," Ψ_0, are more than several electron Larmor radii from the null flux tube.

We also note that since Ψ_0 is a constant of the motion, a particle which enters the null region, although it will in general suffer a change in pitch angle, will retain its gyro-center on the same flux tube once it exits the null. Thus the null introduces no radial particle diffusion even for particles that undergo rapid changes in gyrophase and pitch angle. It is true, however, that an ion which passes over the null saddle point and onto a field line encircling the conductor may suffer a charge exchange event and due to the low resulting ion energy, become trapped on the closed conductor encircling field line.

Appendix B - Equilibrium Pressure Models

The equilibrium models for $\hat{n}$, $\hat{T}$ and $\hat{P}$ in the numerical calculations have the functional form

$$\hat{Q}(\hat{\alpha}) = \frac{(1 + \exp(-\hat{\alpha}_b/\Delta\hat{\alpha}))}{(1 + \exp((\hat{\alpha} - \hat{\alpha}_b)/\Delta\hat{\alpha}))}$$

where $\hat{Q}(\hat{\alpha}) = \hat{n}(\hat{\alpha})$ or $\hat{T}(\hat{\alpha})$ and $\hat{P}(\hat{\alpha}) = \hat{n}(\hat{\alpha})\,\hat{T}(\hat{\alpha})$. The family of pressure profiles for which the marginally stable value of $\hat{\Gamma}$ is plotted in Fig. (7) all have the values $\hat{\alpha}_b = .4$ and $\Delta\hat{\alpha} = .3$ for $\hat{n}$, and $\Delta\alpha = .04$ for $\hat{T}$. The parameter $\hat{\alpha}_b$ in the function for $\hat{T}$ is varied from .7 to .9. The values of $\hat{\alpha}_b$ for the two profiles of ω_* shown in Fig. (6-a) and Fig. (6-b) are .8 and .9 respectively

Acknowledgement

We wish to thank D. Pearlstein for discussions on the analysis of the core stability. We also wish to thank S. DeVoto for the use of the TIBRO particle orbit code. Finally, we wish to acknowledge fruitful discussions with the entire Tara group.

This work was performed under U.S. Department of Energy Contract No. DE-AC02-78ET51013.

References

1. J. Kesner, B.D. McVey, R.S. Post, D.K. Smith, Nucl. Fus 22. 549 (1982).

2. M. Inutake et.al., in Fusion Reactor Design and Technology, (Unipub, New York, 1983), 1, p. 429.

3. R.S. Post, M. Gerver, J. Kesner, J. Irby, B. Lane et.al, Proc 10 Int. Conf. on Plasma Phys. and Cont. Nucl. Fus. Res., London, 1984 (IAEA) Vienna).

4. T. Casper, E.B. Hooper, A. Molvik, A. Sen, in "Summary of TMX-U Results: 1984," LLNL rept. UCID-20274 (1984).

5. S.J. Sackett, "EFFI - A code for calculating the electromagnetic field, force, and inductance in coil systems of evlitary geometry". LLNL Report UCRL - 52402 (1978).

6. M.N. Rosenbluth, N.A. Krall, N. Rostoker, Nucl. Fus. Suppl. 143 (1962).

7. M.N. Rosenbluth and A. Simon, Phy. Fluids 8, 1300 (1965).

8. J. Kesner and B. Lane, Phys. Fluid 28, 634, (1984).

9. B. B. Kadomtsev, in Plasma Physics and the Problem of Controlled Thermonuclear Reactions (Pergamon Press, 1960), **4**, 417.

10. A.Y. Wong, R.W. Schumacher and D.L. Mamas, Comments on Plas. Phys. Cont. Fus **4**, 65 (1978).

Figure Captions

1. Schematic of divertor stabilized tandem mirror showing separatrix flux tube and Modulus - B along a field line passing the null.

2. Detail of experimental divertor coil set showing cross-sections of conductors, field lines and mod B contours. Distances are in centimeters, R=0 is the magnetic axis and Z=0 is the machine midplane.

3. Model equilibrium pressure, density and temperature profiles.

4. Schematic detail of null flux surface showing electron layer, ion layer transition layer and core regions.

5. Schematic diagram of the complex $\hat{\omega}$ plane. The cross hatched region on the negative real axis represents those values of $\hat{\omega}$ which are equal to $\hat{\omega}_*$ at some point in the plasma interior. The bold lines with arrows show the path of the two roots for the n=0 mode as $\hat{\Gamma}$ increased.

6. (a) and (b) $\hat{\omega}_*$ vs. $\hat{\alpha}$ for two closely related pressure profiles. The pressure and density profiles corresponding to Fig. (6-b) are shown in Fig. (4).

7. Marginally stable values of $\hat{\Gamma}$ vs. $\hat{\omega}_*(\hat{\alpha} = 1)/\hat{\omega}_*(\hat{\alpha} = 0)$ for a family of closely related presures profiles. Points labelled (a) and (b) correspond to the pressure profiles for which omega star hat is shown in Fig. (6-a) and Fig. (6-b).

B

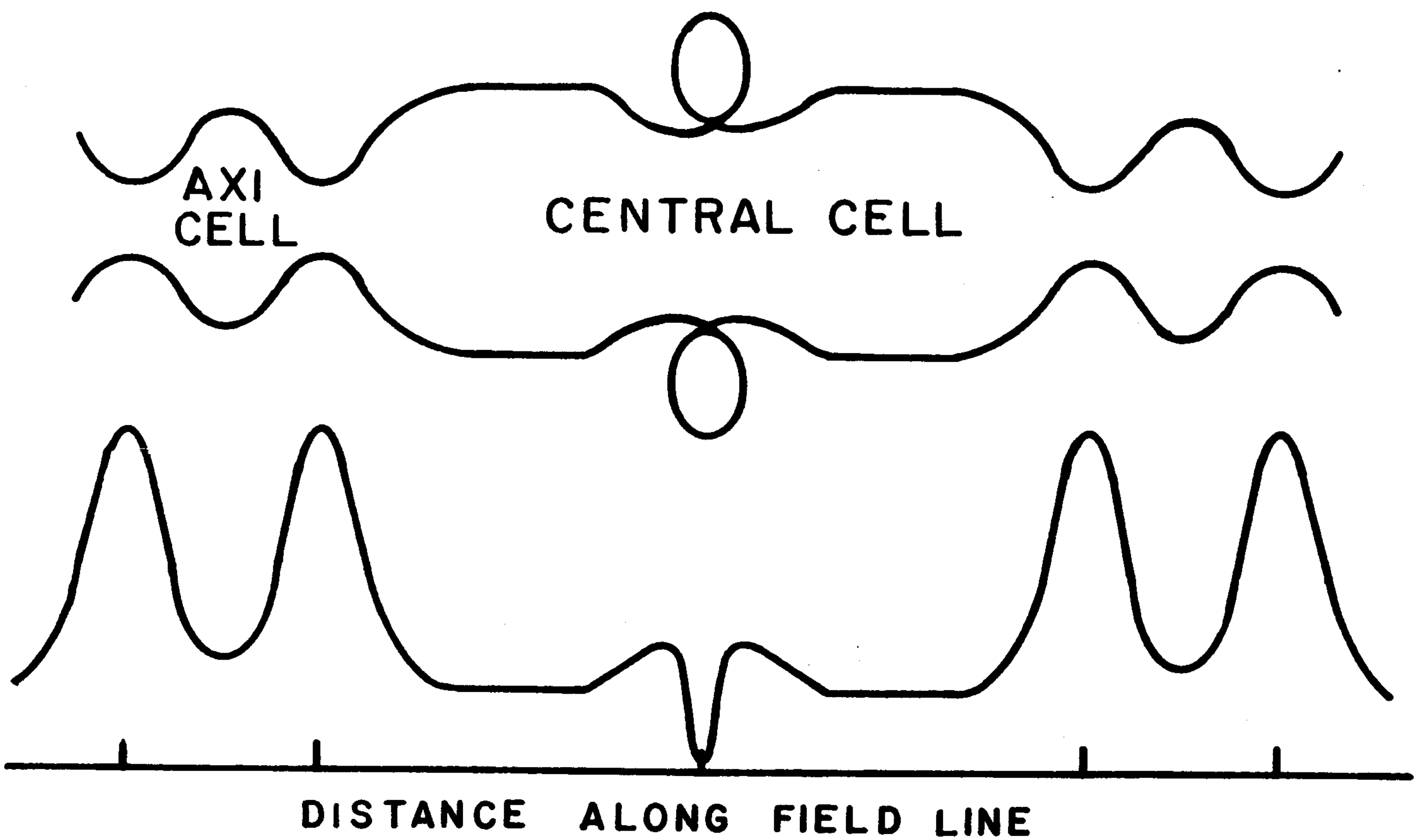

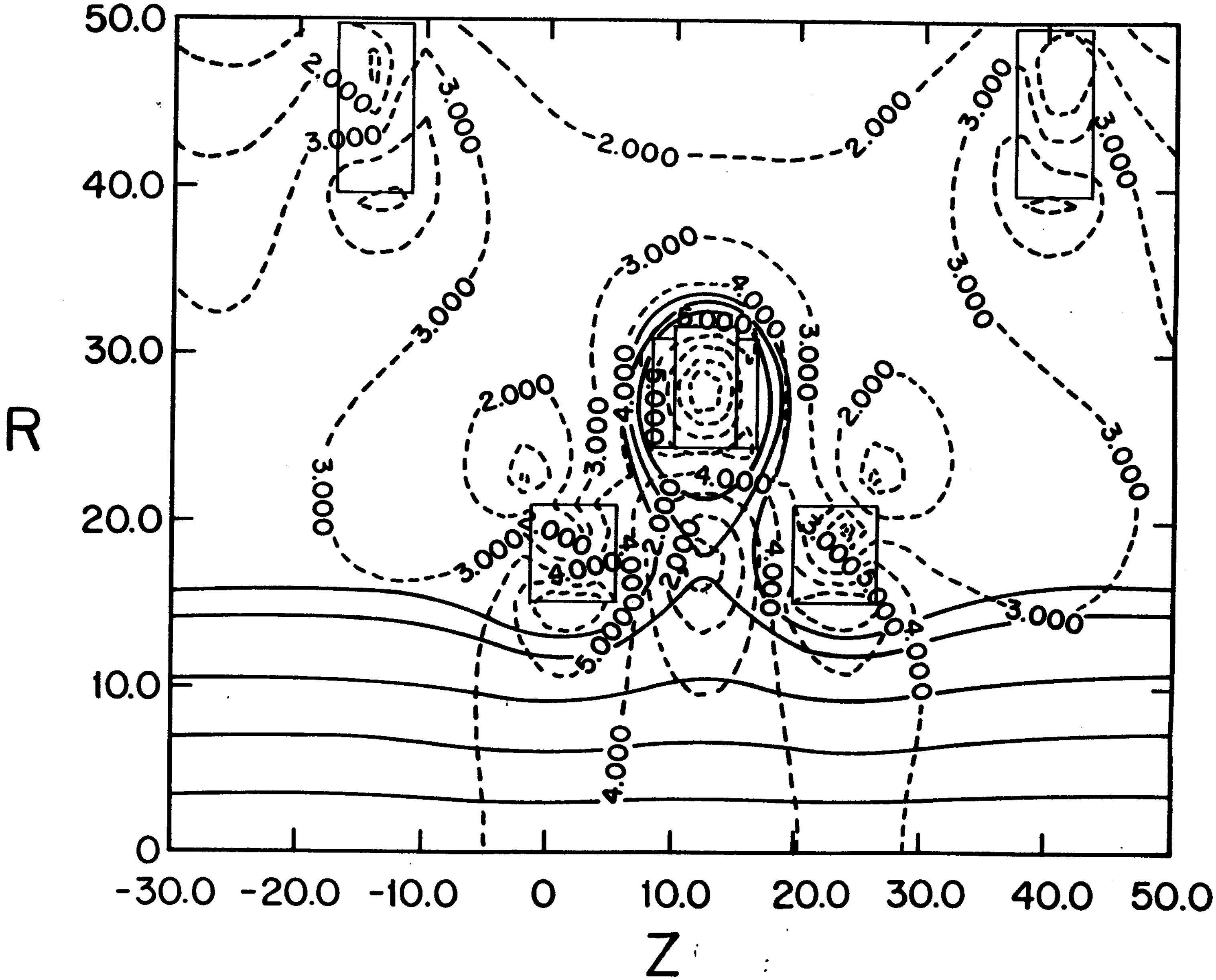
R
Z
50.0
40.0
30.0
20.0
10.0
0
-30.0
-20.0
-10.0
0
10.0
20.0
30.0
40.0
50.0
2.000
3.000
4.000
5.000

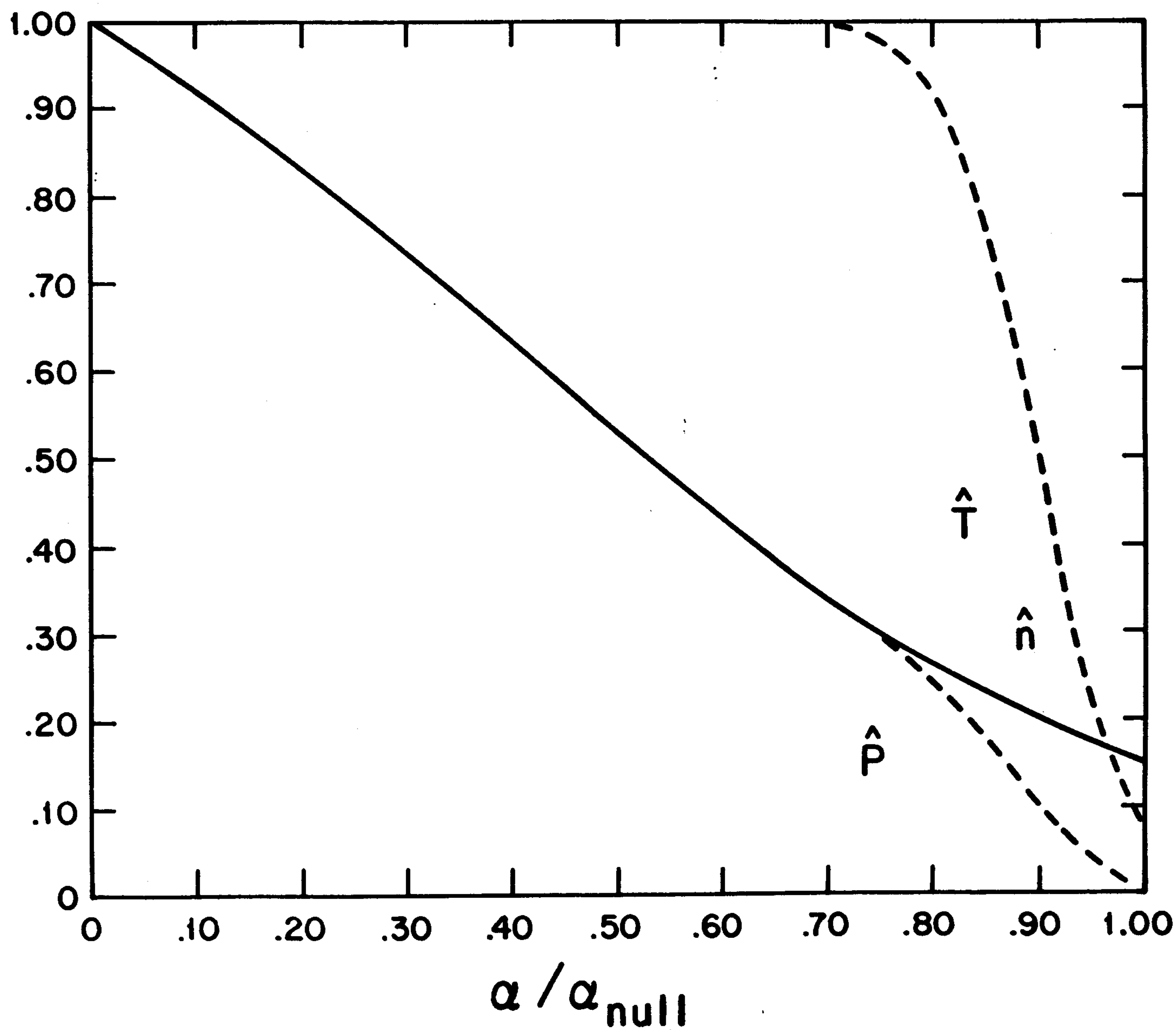

1.00
.90
.80
.70
.60
.50
.40
.30
.20
.10
0
.10
.20
.30
.40
.50
.60
.70
.80
.90
1.00
$\hat{T}$
$\hat{n}$
$\hat{P}$
α / α_{null}

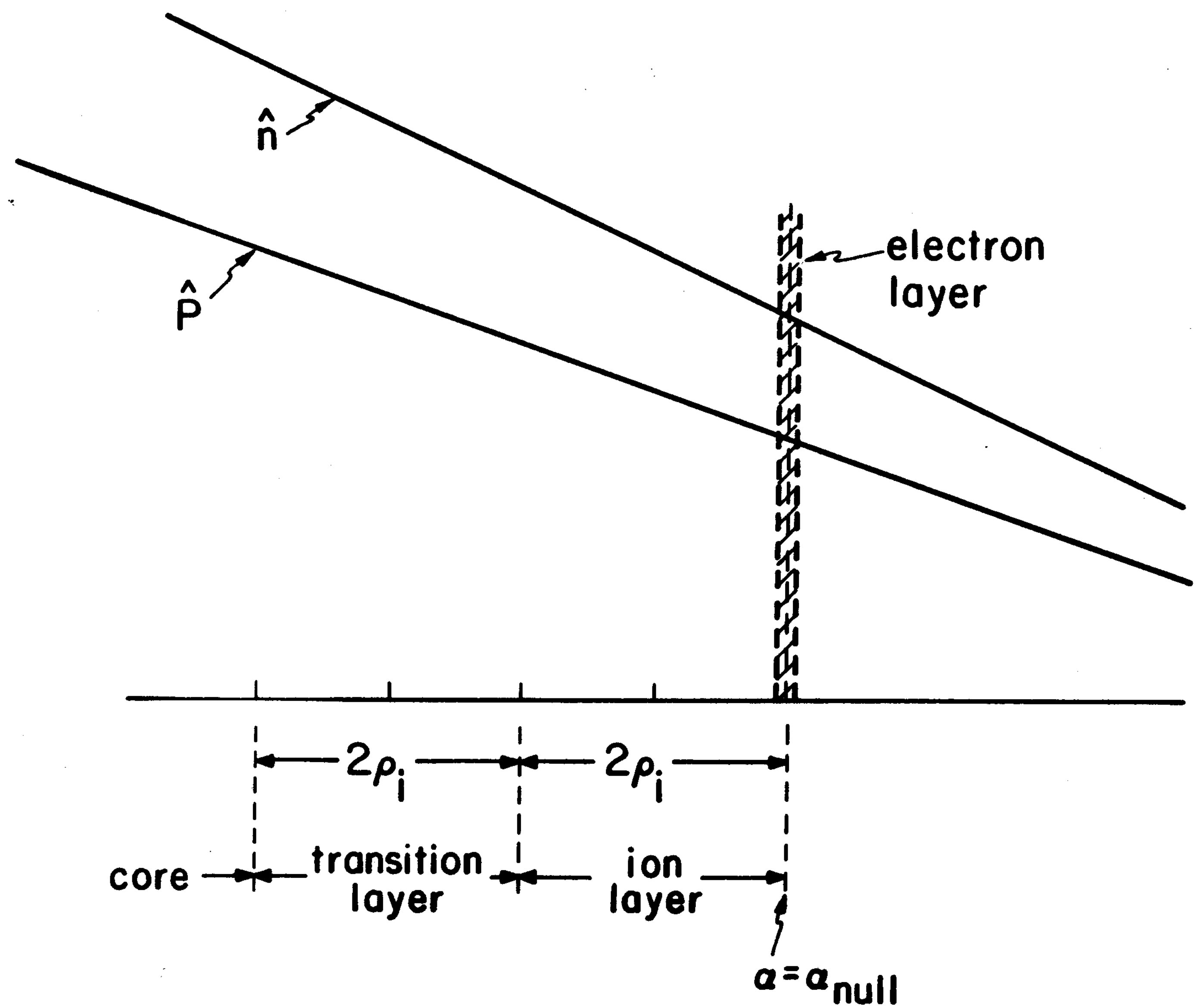

$\hat{n}$
$\hat{P}$
electron layer
$2\rho_i$
$2\rho_i$
core
transition layer
ion layer
$a = a_{null}$

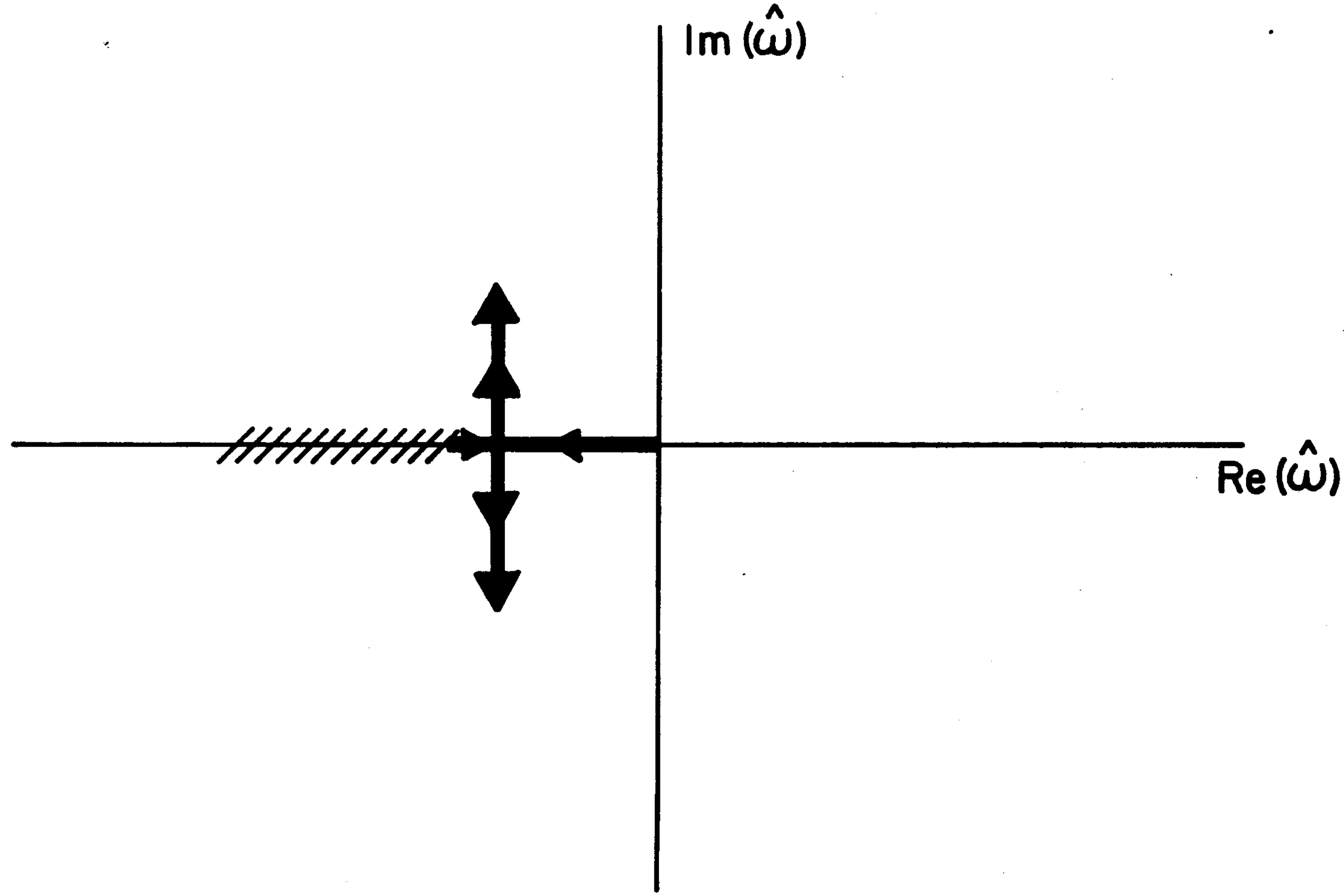

Im ($\hat{\omega}$)
Re ($\hat{\omega}$)

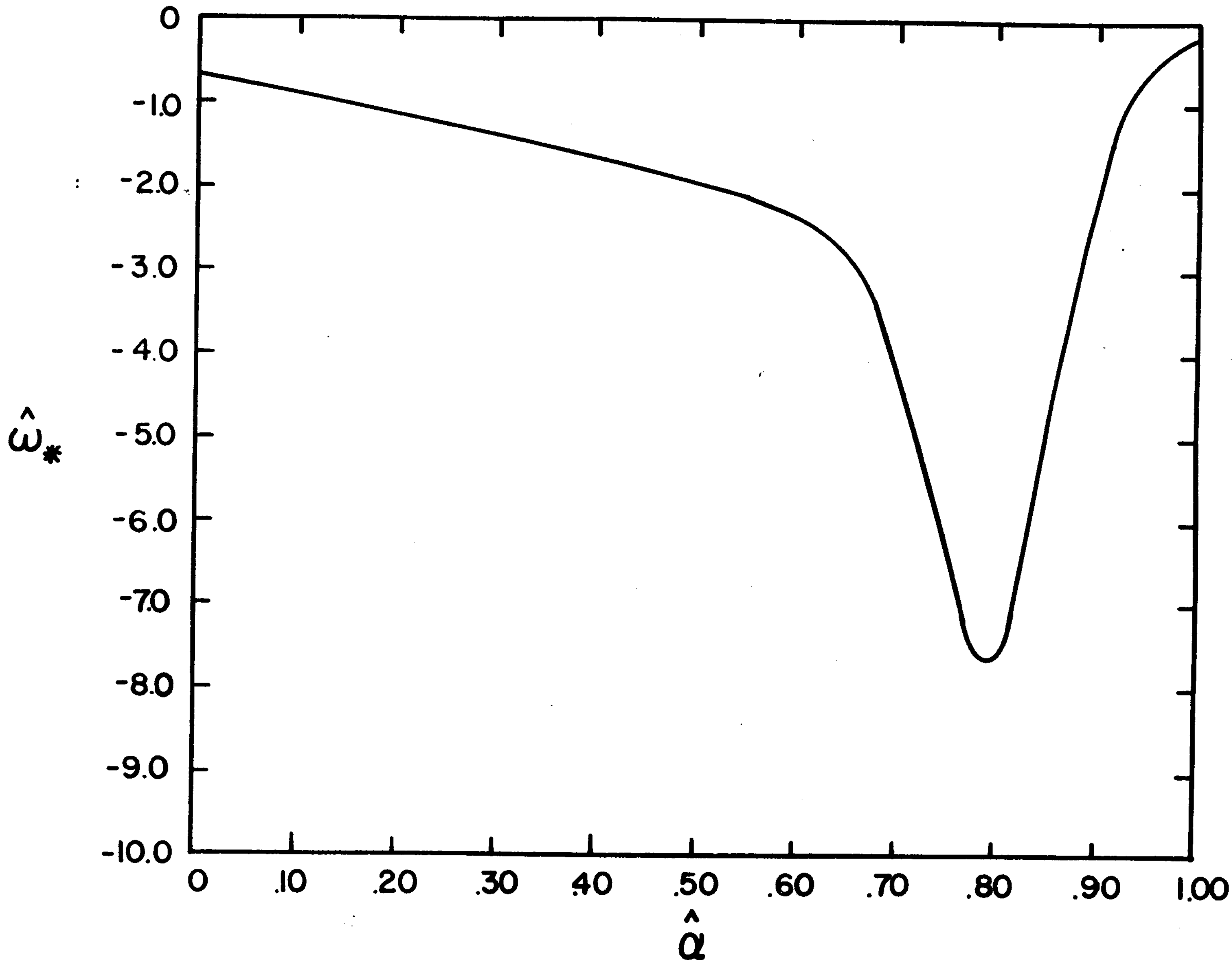

0
-1.0
-2.0
-3.0
-4.0
-5.0
-6.0
-7.0
-8.0
-9.0
-10.0
$\hat{\omega}_*$
0
.10
.20
.30
.40
.50
.60
.70
.80
.90
1.00
$\hat{\alpha}$

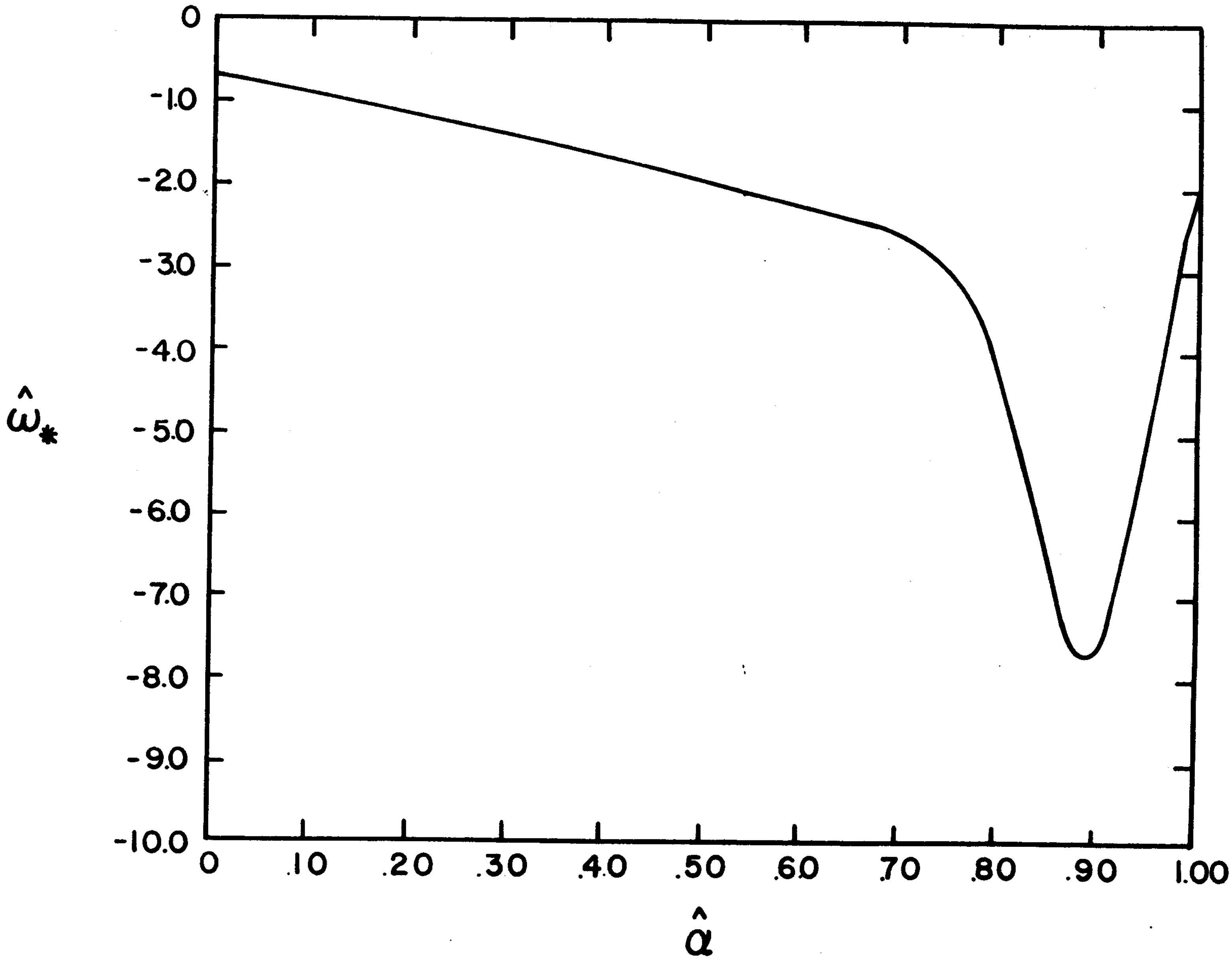

0
-1.0
-2.0
-3.0
-4.0
-5.0
-6.0
-7.0
-8.0
-9.0
-10.0
$\hat{\omega}_*$
0
.10
.20
.30
.40
.50
.60
.70
.80
.90
1.00
$\hat{\alpha}$

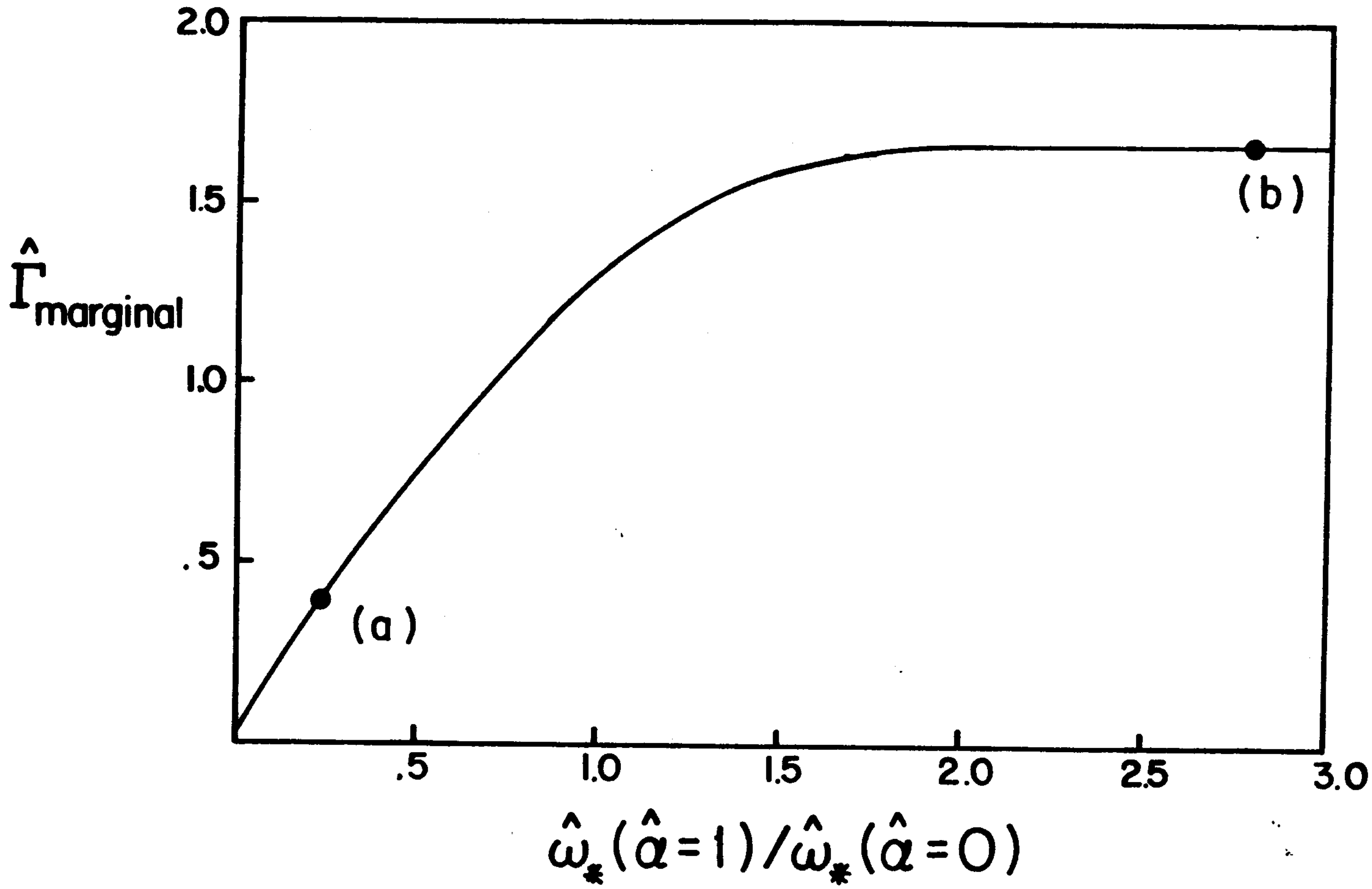

2.0
1.5
1.0
.5
$\hat{\Gamma}_{marginal}$
(a)
(b)
.5
1.0
1.5
2.0
2.5
3.0
$\hat{\omega}_*(\hat{\alpha}=1)/\hat{\omega}_*(\hat{\alpha}=0)$